

RESEARCH ARTICLE

Body weight-dependent troponin T alternative splicing is evolutionarily conserved from insects to mammals and is partially impaired in skeletal muscle of obese rats

Rudolf J. Schilder^{1,*}, Scot R. Kimball¹, James H. Marden² and Leonard S. Jefferson¹

¹Department of Cellular and Molecular Physiology, The Pennsylvania State University College of Medicine, 500 University Drive, Hershey, PA 17033, USA and ²Department of Biology, The Pennsylvania State University, 208 Mueller Lab, University Park, PA 16802, USA

*Author for correspondence (rjs360@psu.edu)

Accepted 19 January 2011

SUMMARY

Do animals know at a physiological level how much they weigh, and, if so, do they make homeostatic adjustments in response to changes in body weight? Skeletal muscle is a likely tissue for such plasticity, as weight-bearing muscles receive mechanical feedback regarding body weight and consume ATP in order to generate forces sufficient to counteract gravity. Using rats, we examined how variation in body weight affected alternative splicing of fast skeletal muscle troponin T (*Tnnt3*), a component of the thin filament that regulates the actin–myosin interaction during contraction and modulates force output. In response to normal growth and experimental body weight increases, alternative splicing of *Tnnt3* in rat gastrocnemius muscle was adjusted in a quantitative fashion. The response depended on weight *per se*, as externally attached loads had the same effect as an equal change in actual body weight. Examining the association between *Tnnt3* alternative splicing and ATP consumption rate, we found that the *Tnnt3* splice form profile had a significant association with nocturnal energy expenditure, independently of effects of weight. For a subset of the *Tnnt3* splice forms, obese Zucker rats failed to make the same adjustments; that is, they did not show the same relationship between body weight and the relative abundance of five *Tnnt3* β splice forms (i.e. *Tnnt3* β 2– β 5 and β 8), four of which showed significant effects on nocturnal energy expenditure in Sprague–Dawley rats. Heavier obese Zucker rats displayed certain splice form relative abundances (e.g. *Tnnt3* β 3) characteristic of much lighter, lean animals, resulting in a mismatch between body weight and muscle molecular composition. Consequently, we suggest that body weight-inappropriate skeletal muscle *Tnnt3* expression in obesity is a candidate mechanism for muscle weakness and reduced mobility. Weight-dependent quantitative variation in *Tnnt3* alternative splicing appears to be an evolutionarily conserved feature of skeletal muscle and provides a quantitative molecular marker to track how an animal perceives and responds to body weight.

Supplementary material available online at <http://jeb.biologists.org/cgi/content/full/214/9/1523/DC1>

Key words: *Tnnt3*, body weight, weight sensing, alternative splicing, troponin T, energetics, metabolic rate, obesity, body composition, skeletal muscle, gastrocnemius, muscle performance.

INTRODUCTION

Skeletal muscles must counteract gravity and adjust their size and/or performance to accommodate variation in body weight. Aside from hypertrophy, the molecular and biochemical mechanisms that muscles use to adjust to changes in body weight are poorly understood, but recent studies in mammals suggest a central role for regulation of sarcomere gene expression (Goldsmith et al., 2010; Kemp et al., 2009). Sarcomere genes encoding proteins that function at the interface between thin and thick filaments are of particular interest, as these play a large role in regulating muscle force output and energy consumption.

One such protein is skeletal muscle troponin T, a component of the troponin complex that regulates muscle contraction and force output (Brotto, 2005; Gomes et al., 2004; Ogut et al., 1999). Mammalian skeletal muscle troponin T is encoded by a slow (*Tnnt1*) and fast (*Tnnt3*) gene (Perry, 1998), the latter of which undergoes extensive alternative splicing. *Tnnt3* pre-mRNA comprises 18 exons, including a cassette of five alternatively spliced exons near the 5' end and a mutually exclusive pair of exons near the 3' end, allowing a possible 128 unique splice forms. Changes in the relative

abundance of different *Tnnt3* alternative splice forms is likely to be an important component of muscle plasticity, as it affects the calcium sensitivity of contraction in isolated striated muscle fibers (Briggs and Schachat, 1996; Brotto, 2005; Gomes et al., 2004; Ogut et al., 1999; Pan and Potter, 1992).

Alternative splicing of troponin T in mammals has been studied primarily in regard to qualitative shifts in protein isoform expression during early development, and in response to altered muscle use (Medford et al., 1984; Perry, 1998; Stefancsik et al., 2003; Stevens et al., 2003; Yu et al., 2006). A recent study of insect flight muscles demonstrated that there is precise quantitative variation in the relative abundance of alternatively spliced troponin T mRNA transcripts and protein isoforms in response to experimental manipulation of body weight and nutritional state (Marden et al., 2008). Here, we used rats to test the hypothesis that in a mammalian load-bearing (gastrocnemius) muscle, quantitative alternative pre-mRNA splicing of *Tnnt3* is similarly regulated in response to natural and experimentally imposed variation in body weight.

In addition to responding to body weight, the troponin T mRNA splice form profile in insect flight muscle is associated with

metabolic rate during activity (Marden et al., 2008). This is consistent with the known effects of troponin T isoforms on muscle fiber force output in both insects and mammals (Chandra et al., 2006; MacFarland et al., 2002; Marden et al., 2001; Marden et al., 1999; Nassar et al., 2005), which presumably affect the rate of ATP consumption (Greaser et al., 1988). How variation in troponin T alternative splicing relates to mammalian muscle energetics *in vivo* is unknown. Hence, we tested the hypothesis that quantitative variation in *Tnnt3* splice form abundance in rat gastrocnemius muscle is associated with differences in *in vivo* energy expenditure.

Mammalian obesity involves extreme weight gain and a possible failure of body weight homeostasis. There are deficits in skeletal muscle function in obesity (Hulens et al., 2001; Jackson et al., 2009; Lafortuna et al., 2005), accompanied by reduced physical activity and energy expenditure (Galgani and Ravussin, 2008; Goldsmith et al., 2010; Larson et al., 1995; Rosenkilde et al., 2010), phenotypes which may further exacerbate the obese etiology. Root causes of such deficits may originate from within the contractile apparatus, but little is known about the way skeletal muscle composition changes as body weight increases during the development of obesity. We therefore tested the hypothesis that the *Tnnt3* alternative splicing response to changing body weight is impaired during the development of obesity in the Zucker rat, a genetic model of mammalian obesity.

MATERIALS AND METHODS

Animals

Male Sprague–Dawley (strain 400) and Zucker rats (CrI:ZUC-*Lepr^{fa/fa}*, strain 185 and CrI:ZUC-*Lepr^{Fa/x}*, strain 186) were purchased from Charles River Laboratories International, Inc. (Horsham, PA, USA). In all experiments, animals were given *ad libitum* access to water and a Teklad 8604 Rodent Diet (Harlan Inc., Indianapolis, IN, USA), containing 24% protein and 4.5% fat per total mass. Animals were housed individually in flat-bottomed cages containing soft bedding. To ensure that the animals had full access to food and water, food pellets were placed on the bottom of the cage and extra-long sipper tubes were attached to water bottles. Individual food consumption was monitored throughout these experiments and after recovery from anesthesia, and showed no lasting abnormalities associated with the treatments.

Manipulation of body weight

To increase skeletal muscle loading, rats were briefly anesthetized using isoflurane, and fitted with a custom-made vest held in place by Tygon tubing placed around the shoulders and lower abdomen. The vest consisted of a narrow, semi-flexible plate, worn dorsally, to which two elastic pouches, one each side of the spine, were firmly attached by means of Velcro. Control rats carried a vest without weights, or no vest at all. In randomly selected individuals, the pouches were filled with an equal number of lead spheres (~1 g each) and secured by the Tygon tubing. Weight loads varied from 5 (vest only) to 90 g. Body mass was defined as the post-experiment body mass of animals without weight loads. Total mass was defined as the native body mass plus vest mass. Rats wore vests for 5 days, after which the vest and body mass were measured. The body mass of obese and lean Zucker rats was not experimentally manipulated, and is therefore equivalent to total mass. In all, we collected samples from 50 male Sprague–Dawley, nine lean Zucker and nine obese Zucker rats varying in total mass from approximately 90 to 400 g, with experimental loads comprising 28–36% of body mass. Rats were anesthetized using isoflurane, after which gastrocnemius

muscles were dissected and flash frozen in liquid nitrogen until further use. Rats were killed post-dissection. This protocol was approved by the Institutional Animal Care and Use Committee at The Pennsylvania State University College of Medicine.

Energy expenditure, activity and body composition

Weight-loaded and control rats were placed in metabolic chambers for 5 days, under 12 h light/dark regimes. Oxygen consumption (\dot{V}_{O_2}) and respiratory exchange ratio (RER) throughout the 5 day period were obtained using an Oxymax open circuit indirect calorimetry system (Columbus Instruments, Columbus, OH, USA), with airflow of 2.51 min^{-1} . Data were collected from each chamber for 1 min at 15 min intervals. Ambulatory activity was determined using an Opto M3 system (Columbus Instruments) that measured optical beam breaks in both the horizontal and vertical direction. Mean ambulatory activity was defined as the mean total sequential horizontal beam breaks per 15 min measuring interval. Body composition was measured in a subset of the live Sprague–Dawley and Zucker rats with a Bruker Minispec LF90 NMR Analyzer (Bruker Optics, Inc., Billerica, MA, USA) immediately before gastrocnemius muscle dissection. Briefly, rats were weighed, immobilized in a Plexiglas cylinder, and placed inside the Minispec for approximately 1 min. During this time measurements of whole body fat and lean (muscle) mass content were obtained using manufacturer-recommended rat-specific acquisition parameters.

Tnnt3 splice form characterization and quantification of splice form relative abundance

Total RNA was extracted from gastrocnemius muscle using Trizol reagent (Invitrogen, Carlsbad, CA, USA), and precipitated in isopropanol, according to the manufacturer's instructions. Total RNA was reverse transcribed using a High Capacity cDNA Reverse Transcription kit (Applied Biosystems, Foster City, CA, USA). *Tnnt3* amplicons were amplified by PCR using fluorescein (FAM)-labeled forward primer, fTnt_F1 (5'-FAM-CCCCAACCTTCTCAGACT-3'), and two unlabeled reverse primers, fTnt_R2 (5'-CCTTCT-TGCTGTGCTTCTGG-3') and fTnt_R4 (5'-CGGACAGTCAT-GATATCGTATT-3'). Forward primer fTnt_F1 hybridizes to the *Tnnt3* 5' UTR, 28 nucleotides upstream of the start codon. The 5' alternative exon cassette starts 27 nucleotides downstream of the start codon. Reverse primer fTnt_R2 sequence spans constitutive exon 18 and 3' alternative exon 17, whereas fTnt_R4 spans 3' alternative exon 16 and constitutive exon 15 (Fig. 1). Using this amplification strategy, all of the possible alternative *Tnnt3* mRNA splice form amplicons had a unique size, with a minimum length difference of three nucleotides. PCR was performed using HotStart GoTaq polymerase (Promega, Madison, WI, USA) under the following cycling conditions: 5 min at 95°C, followed by 4 cycles of 30 s at 94°C, 30 s at 65°C (–1.0°C/cycle), followed by 1 min, 15 s at 72°C. This was followed by 29 cycles of 30 s at 94°C, 30 s at 60°C, 1 min and 15 s at 72°C, with a final 15 min at 72°C to end.

For quantitative analyses of *Tnnt3* splice form relative abundance in individual muscle samples, FAM-labeled PCR products were diluted 1:25 and 1 µl of this dilution was analyzed by capillary electrophoresis (ABI DNA Analyzer, Applied Biosystems). Any samples with a fragment peak height exceeding the linear detection range of the instrument were further diluted and run again. Relative abundance of each amplicon in the PCR reaction was determined by dividing its peak height by the total of all peak heights (see Fig. 1B). Amplicon fragment size was determined using an internal size standard and Genemapper® (Applied Biosystems) fragment analysis software.

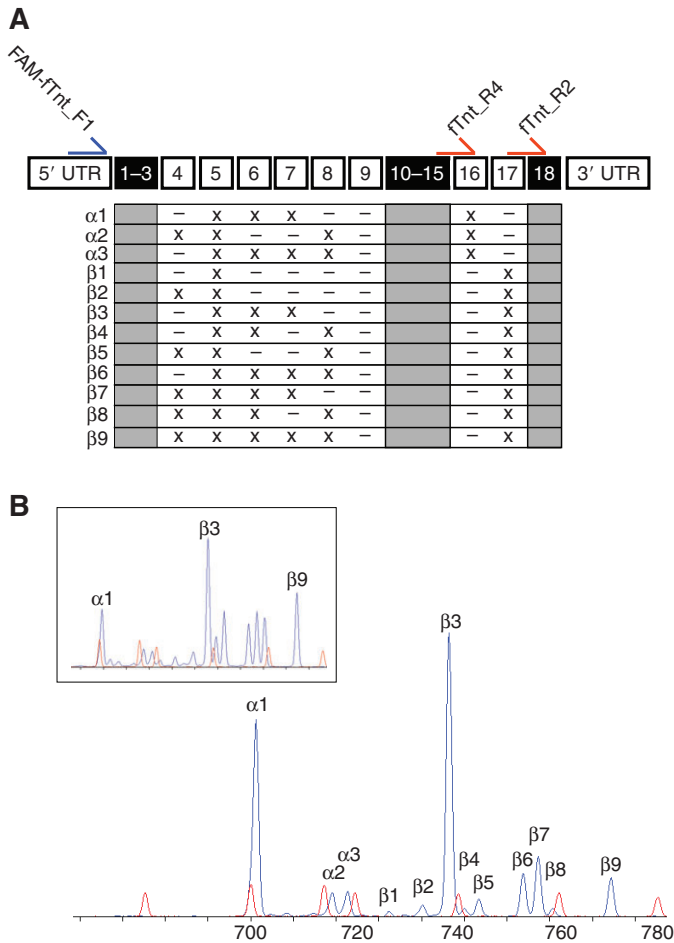


Fig. 1. Characterization and quantification of *Tnnt3* alternative splicing in rat gastrocnemius muscle. (A) Rat *Tnnt3* pre-mRNA comprises 18 exons, including a 5' alternatively spliced cassette containing exons 4–9 (white boxes), and the mutually exclusive exons 16 and 17. Twelve different *Tnnt3* splice forms were detected by RT-PCR and cDNA sequencing ('X' denotes inclusion of specific exons). Forward (FAM-fTnt_F1, blue) and reverse (fTnt_R2 and fTnt_R4, red) RT-PCR primers were designed so that each possible *Tnnt3* splice form amplicon size was unique and detectable by DNA fragment analysis (see Materials and methods). Splice forms containing exon 16 or exon 17 were given an ' α ' or ' β ' designation, respectively. (B) Fluorescently labeled DNA fragment peaks showing *Tnnt3* splice form diversity and abundance (i.e. peak height) of each splice form in gastrocnemius muscle of two rats differing in size (inset shows spectrum for the smaller of the two rats). Internal size standards are represented by red traces.

Nucleotide sequences were confirmed by cloning and sequencing each of the uniquely sized amplicons from PCR amplification of cDNA pooled from gastrocnemius muscles of a number of different-sized Sprague–Dawley rats. This amplicon pool was extracted from an agarose gel using a QiaQuick gel extraction kit (Qiagen, Valencia, CA, USA), cloned using a TOPO-TA cloning kit (Invitrogen) and sequenced (ABI Hitachi 3730XL DNA Analyzer, Applied Biosystems).

Tnnt3 protein (TNNT3) expression

Myofibrillar protein homogenates were prepared from flash-frozen gastrocnemius muscle samples as described previously (Hartner et al., 1989). The protein concentration of homogenates was determined (Bradford reagent, Bio-Rad, Hercules, CA, USA) and 15 μ g of total protein per sample was loaded onto a 14% SDS-PAGE gel

(acrylamide/bisacrylamide ratio 30:0.19). Electrophoretically separated proteins were transferred onto PVDF membranes, which were subsequently probed with a polyclonal anti-fast skeletal muscle troponin T antibody (C-18, Santa Cruz Biotechnology, Inc., Santa Cruz, CA, USA). TNNT3 protein bands were visualized using chemiluminescence (ECL PlusTM, GE Healthcare, Chalfont St Giles, Bucks, UK) and a GeneGnome imaging system (Syngene, Frederick, MD, USA). Blots were stripped for 30 min at 55°C, in 0.063 mol l⁻¹ Tris-HCl, 0.07 mol l⁻¹ sodium dodecyl sulfate (SDS) and 0.11 mol l⁻¹ β -mercaptoethanol, pH 6.7, and reprobbed with a monoclonal β -actin antibody (Sigma A5060, St Louis, MO, USA). Background-corrected, integrated optical band densities were quantified with Genetools (Syngene) software. Individual TNNT3 protein band abundance was expressed relative to the total abundance of all detected TNNT3 protein bands per sample. We also quantified β -actin protein abundance; this quantity was included in a statistical analysis to verify that covariance between relative abundance of TNNT3 isoforms and body mass occurred independently of variation in other sarcomere proteins and was not an artefact of differences in gel loading (see supplementary material Table S1).

RESULTS

Alternative splicing of rat skeletal muscle *Tnnt3*

We detected 12 mature *Tnnt3* splice forms expressed in rat skeletal muscle (see Fig. 1A for the exon structure of each splice form) by means of RT-PCR screening of total RNA. Sequencing of cDNA clones showed that 9 of the 12 distinct mRNA splice forms contained exon 17 (henceforth referred to as *Tnnt3* $\beta 1$ – $\beta 9$), and three contained exon 16 (henceforth referred to as *Tnnt3* $\alpha 1$ – $\alpha 3$; Fig. 1A). These results are consistent with previous findings regarding the *Tnnt3* splice forms expressed in adult mammalian skeletal muscle (Briggs and Schachat, 1996), but extend considerably the known number of *Tnnt3* mRNA splice forms expressed in adult rodent muscle. To our knowledge, only seven adult *Tnnt3* mRNA splice forms have been reported previously (Wang and Jin, 1997).

Effects of weight manipulation on *Tnnt3* splicing

Weight loads caused pronounced effects on the *Tnnt3* mRNA splice form relative abundance, whereas wearing the unweighted vest had little if any effect (Table 1). The first principal component of variation in *Tnnt3* splice form relative abundance, characterizing the overall splice form mixture, was significantly related to body mass ($F=101.2$, $P<0.0001$) and weight load ($F=22.3$, $P<0.0001$). Individually, 8 out of 12 *Tnnt3* mRNA splice forms responded to total mass, with body mass and weight load showing highly significant additive effects (Table 1). For example, the *Tnnt3* $\alpha 1$ relative abundance in weight-loaded rats was indistinguishable from that in unloaded rats of the same total mass (Fig. 2A). Not all splice forms responded to weight in the same fashion (Fig. 2B), as certain ones (e.g. *Tnnt3* $\beta 2$; Fig. 2B) were completely non-responsive to weight. *Tnnt3* $\beta 3$ showed a mixed response, increasing in relative abundance in rats weighing ~100–250 g, but with no further increase at higher body mass.

Weight-dependent changes in *Tnnt3* expression were also evident at the protein level, albeit less well resolved given the complexity of the isoform mixture. The relationship between body mass and the relative abundance of the two most abundant TNNT3 bands (bands 2 and 4 in Fig. 3A) followed the same pattern as the two most abundant mRNA splice forms (i.e. *Tnnt3* $\beta 3$ and *Tnnt3* $\alpha 1$; compare Fig. 2 and Fig. 3B). Thus, although we did not fully characterize these protein bands, there were clear body weight-associated shifts in relative TNNT3 band abundance that correlated with the more readily measured changes at the mRNA level.

Table 1. *F*-statistics and associated *P*-values for effects of body mass, weight load and presence of a vest on *Tnnt3* splice form relative abundance

<i>Tnnt3</i> splice form	Model effects					
	Body mass		Weight load		Vest (yes/no)	
$\alpha 1$	90.5	(<0.0001)	27.30	(<0.0001)	2.20	(0.15)
$\alpha 2$	27.1	(<0.0001)	7.10	(0.01)	1.40	(0.25)
$\alpha 3$	13.2	(0.0007)	9.20	(0.004)	2.10	(0.16)
$\beta 1$	41.2	(<0.0001)	6.20	(0.016)	1.40	(0.25)
$\beta 2$	1.5	(0.23)	0.67	(0.42)	0.31	(0.58)
$\beta 3$	32.4	(<0.0001)	0.06	(0.81)	3.03	(0.09)
$\beta 4$	0.07	(0.80)	5.48	(0.024)	5.25	(0.03)
$\beta 5$	62.9	(<0.0001)	3.86	(0.055)	0.05	(0.82)
$\beta 6$	14.3	(0.0004)	15.30	(0.0003)	0.38	(0.54)
$\beta 7$	21.0	(<0.0001)	3.18	(0.08)	0.04	(0.85)
$\beta 8$	22.7	(<0.0001)	6.24	(0.016)	7.83	(0.0075)
$\beta 9$	104.2	(<0.0001)	10.95	(0.0018)	3.40	(0.07)
PC1	101.2	(<0.0001)	22.3	(<0.0001)	3.9	(0.06)

Results of ANCOVA models ($N=50$, $\alpha=0.05$) predicting the effects of body mass, added weight load and presence of a vest on relative *Tnnt3* splice form abundance (d.f.=1 for each predictor) in male Sprague–Dawley rats. *P*-values are given in parentheses.

Significant *P*-values for body mass indicate that *Tnnt3* splice form abundance responds to natural variation in body mass.

Significant *P*-values for weight load indicate that, independently of natural body mass variation, *Tnnt3* splice form abundance responds to experimental manipulation of body weight.

The bottom row shows that both body mass and added weight load are highly significant predictors of the first principal component (PC1) of the *Tnnt3* splice form relative abundance.

Tnnt3 splice form abundance is associated with energy expenditure during activity

Changes in *Tnnt3* splice form abundance in response to weight loading were not associated with gross alterations in activity or

energy expenditure (Fig. 4), as weight-loaded and control rats showed no differences in ambulatory activity, energy expenditure ($\dot{V}O_2$) or RER (i.e. $\dot{V}CO_2/\dot{V}O_2$). Moreover, a multiple regression model showed that ambulatory activity was not significantly associated

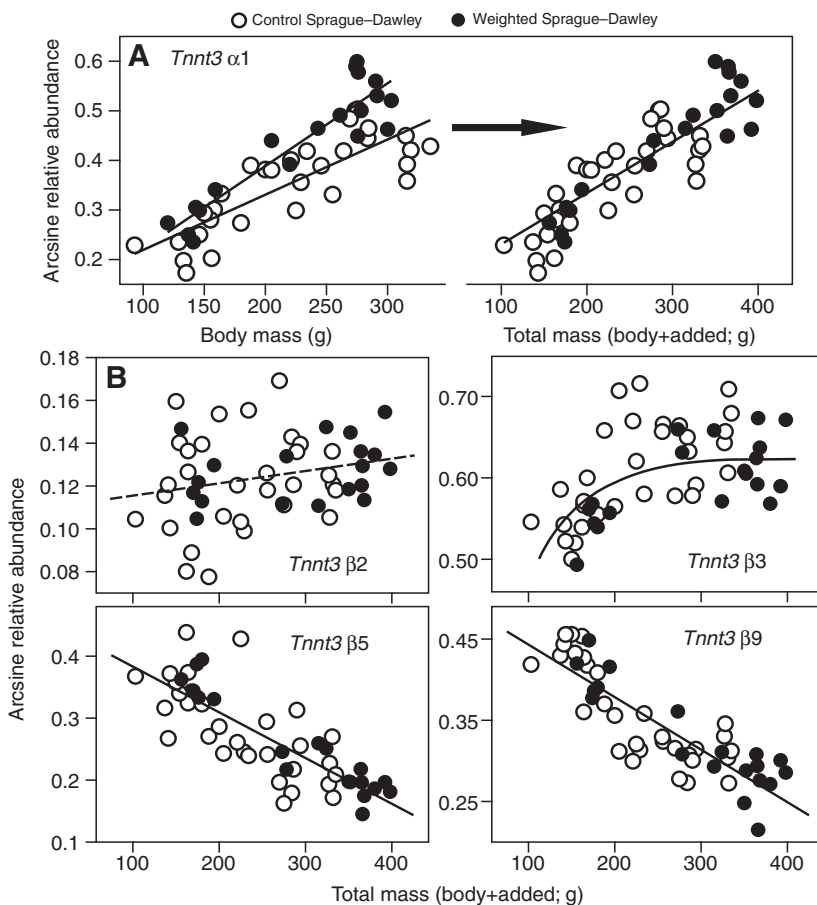


Fig. 2. *Tnnt3* splice form abundance is adjusted to total mass in rat gastrocnemius muscle. (A) Relative abundance of *Tnnt3* splice form $\alpha 1$ as a function of native body mass (left) and total mass (body+added load; right) for weight-loaded and control male Sprague–Dawley rats. Solid lines depict linear regression fits to data for weight-loaded ($R^2=0.84$, $P<0.0001$, $N=19$) and control animals ($R^2=0.67$, $P<0.0001$, $N=31$), separately (left panel) or combined (right panel) ($R^2=0.78$, $P<0.0001$). (B) Expression of *Tnnt3* splice form $\beta 2$ (plotted here against total load) was not sensitive to native or experimental changes in body weight. *Tnnt3* splice form $\beta 3$ expression initially increased with total mass, but leveled off in rats >250 g. Both *Tnnt3* $\beta 5$ and $\beta 9$ expression correlated negatively with total mass and were sensitive (*Tnnt3* $\beta 5$ marginally so) to experimental body weight manipulation (see Table 1). All relative abundance data were arcsine transformed to achieve normality.

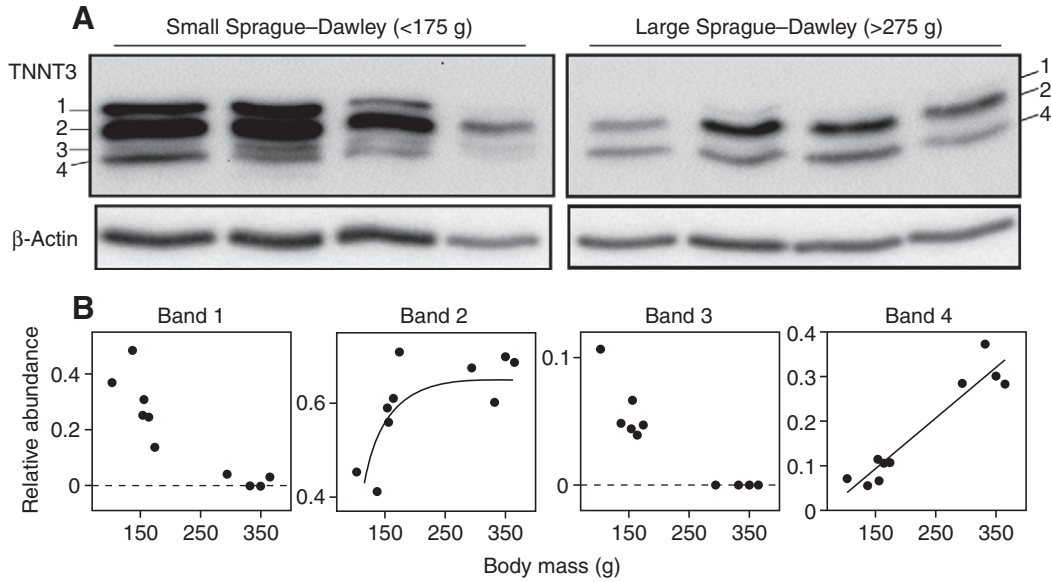


Fig. 3. Weight-associated changes in TNNT3 protein bands. (A) A western blot for TNNT3 detected four bands in smaller Sprague-Dawley rats, whereas three bands (i.e. bands 1, 2 and 4) were apparent in larger rats. β -Actin levels (obtained after stripping and reprobing the same western blot) are provided to demonstrate relatively uniform protein loading. β -Actin levels were not significantly affected by changes in body weight (one-way ANOVA: $F=2.57$, $P=0.163$). (B) Relative abundance of TNNT3 protein bands in relation to body mass. In a sample of gastrocnemius muscles from 10 Sprague-Dawley individuals, the most abundant TNNT3 protein (band 2) matched the behavior of the most abundant mRNA splice form (*Tnnt3* β 3; Fig. 2B) in regard to its relationship with body mass (i.e. increasing at low body mass and leveling off above 250 g). The second most abundant TNNT3 protein, band 4, and the second most abundant mRNA splice form, *Tnnt3* α 1 (Fig. 2A), in large rats showed the same linear increase with body mass. These trends associated with body mass increase were evident when variation associated with protein loading was taken into account as a three-way ANOVA (i.e. with TNNT3 band relative abundance as responses, and total TNNT3 band density, β -actin density and body mass as factors) revealed significant effects of body mass only (supplementary material Table S1).

with either rat size (body mass; $F=2.21$, $P=0.16$) or the amount of weight load ($F=0.11$, $P=0.75$).

To more closely examine the effect of the *Tnnt3* splice form profile on energy expenditure, we controlled for individual differences that would otherwise inflate the error variance and reduce statistical power. In this analysis, the response variable was night-

time \dot{V}_{O_2} , the period when rats were most active. We included as independent variables the day-time \dot{V}_{O_2} , to account for individual variation in size and resting metabolic rate, and night-time ambulatory activity to control for activity level (Table 2). The relative abundance of *Tnnt3* splice forms had significant independent effects on night-time \dot{V}_{O_2} independently of weight load (Table 2). Rats with

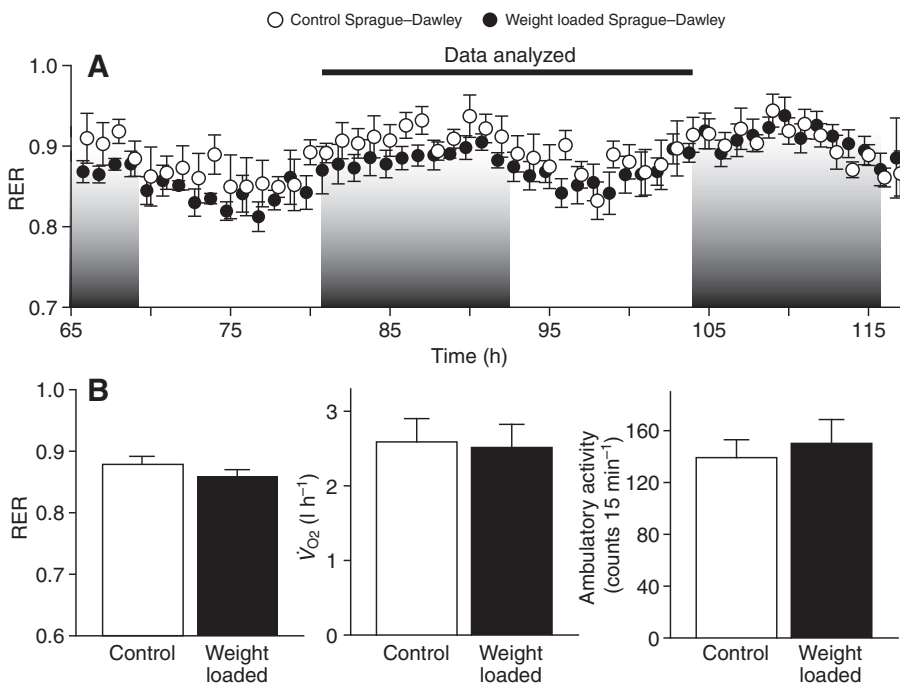


Fig. 4. Experimental manipulation of body weight did not affect metabolism, locomotor activity or energy expenditure. (A) Mean respiratory exchange ratio (RER, i.e. $\dot{V}_{CO_2}/\dot{V}_{O_2}$) as a function of time for weight-loaded and control rats maintained in indirect calorimetry chambers for 5 days, during the last ~50 h of the experiment ($N=16$ rats). Shaded areas indicate the dark period of the 12h light/dark cycle. Statistical analyses of the effects of weight loading on energy expenditure and activity (see also Table 3) were performed on data obtained during the last full day (i.e. animals had been weight loaded for 4 days). (B) Comparison of mean RER (0.88 ± 0.009 vs 0.86 ± 0.01), mean \dot{V}_{O_2} (2589.3 ± 312.2 vs $2514.2\pm 310.2\ ml\ h^{-1}$) and mean ambulatory activity (139.2 ± 13.8 vs 150.2 ± 18.5 counts $15\ min^{-1}$) during day 4. No differences were detected between weight-loaded and control animals. Means are presented with s.e.m. (error bars).

Table 2. *F*-statistics and associated *P*-values for effects of night-time ambulatory activity and weight load, and the relative abundance of each of 12 *Tnnt3* splice forms on mean night-time \dot{V}_{O_2}

<i>Tnnt3</i> splice form	Model effects						
	Relative abundance			NAA		Weight load	
$\alpha 1$	10.50	(0.008)	+	0.5	(0.5)	5.6	(0.04)
$\alpha 2$	4.71	(0.053)		0.030	(0.9)	1.9	(0.2)
$\alpha 3$	0.91	(0.36)		0.003	(0.96)	0.6	(0.4)
$\beta 1$	10.61	(0.008)	–	1.82	(0.20)	5.1	(0.045)
$\beta 2$	0.02	(0.90)		0.002	(0.97)	0.02	(0.9)
$\beta 3$	9.22	(0.01)	+	0.007	(0.93)	0.34	(0.5)
$\beta 4$	6.21	(0.03)	–	0.1	(0.8)	3.5	(0.09)
$\beta 5$	4.04	(0.07)		0.005	(0.94)	0.98	(0.34)
$\beta 6$	0.47	(0.51)		0.09	(0.8)	0.4	(0.5)
$\beta 7$	7.43	(0.02)	–	0.01	(0.92)	2.1	(0.2)
$\beta 8$	8.76	(0.013)	–	0.000	(0.995)	2.9	(0.12)
$\beta 9$	10.89	(0.007)	–	0.002	(0.97)	4.1	(0.07)
PC1	9.80	(0.0097)		0.14	(0.72)	4.8	(0.05)

Results of multiple regression models ($N=16$, $\alpha=0.05$; *P*-values are given in parentheses) for energy expenditure during activity (i.e. mean night-time \dot{V}_{O_2}), using weight load and each *Tnnt3* splice form as predictors (d.f.=1, for all predictors). Also included in each of these models were night-time ambulatory activity (NAA) and mean daytime \dot{V}_{O_2} . *P*-values for the latter were omitted from this table ($P<0.0001$ for all nine models), as this factor was primarily included to account for size-dependent variation in resting metabolic rate.

Significant *P*-values for a *Tnnt3* splice form indicate that its relative abundance affects energy expenditure during activity, independently of weight, NAA and mean daytime \dot{V}_{O_2} .

The + and – designations in the *Tnnt3* splice form relative abundance column represent the directionality of the splice form-specific effects on mean night-time \dot{V}_{O_2} .

The bottom row shows that both the first principal component (PC1) of the *Tnnt3* splice form relative abundance and weight load had independent, significant effects on energy expenditure during activity.

muscles containing more *Tnnt3* $\alpha 1$ and $\beta 3$ at a given daytime \dot{V}_{O_2} and weight load expended energy at a higher rate (see directionality of effects in Table 2), as expected if the functional effect of expressing proportionately more of these splice forms increases force and power. *Tnnt3* $\alpha 1$ and $\beta 3$ are among the smaller *Tnnt3* splice forms and have identical 5' exon composition (Fig. 1A), and hence these energetic results are consistent with a previous qualitative finding that unloaded soleus muscles [hindlimb-suspended rats (Yu et al., 2006)] had reduced expression of smaller *Tnnt3* isoforms and

produced less force (i.e. opposite to the effects we observed in response to weight loading).

Regulation of *Tnnt3* alternative splicing is impaired in obese rats

Fat loads of obese Zucker rats in relation to lean mass were similar to the exogenously applied loads in the foregoing experiment (ANCOVA *post hoc* Student's *t*-test: $\alpha=0.05$, $t=0.96$, $P=0.34$; Fig. 5B) and hence the skeletal muscles were loaded in a comparable

Table 3. *F*-statistics and associated *P*-values for effects of body mass, Zucker rat strain and interaction term on *Tnnt3* splice form relative abundance

<i>Tnnt3</i> splice form	Model effects					
	Body mass		Obese/lean		Body mass \times obese/lean	
$\alpha 1$	90.5	(<0.0001)	27.30	(<0.0001)	2.20	(0.15)
$\alpha 1$	11.7	(0.003)	0.45	(0.5)	0	(0.998)
$\alpha 2$	0.32	(0.58)	0.45	(0.5)	0.001	(0.97)
$\alpha 3$	0.02	(0.9)	0.5	(0.5)	0.11	(0.74)
$\beta 1$	21.1	(0.0002)	0.1	(0.8)	8.1	(0.01)
$\beta 2$	6.0	(0.02)	3.9	(0.06)	0.07	(0.80)
$\beta 3$	36.8	(<0.0001)	80.6	(<0.0001)	9.1	(0.007)
$\beta 4$	1.4	(0.3)	12.4	(0.002)	5.2	(0.03)
$\beta 5$	13.4	(0.002)	3.8	(0.007)	9.8	(0.005)
$\beta 6$	36.6	(<0.0001)	0.32	(0.58)	0.97	(0.34)
$\beta 7$	7.99	(0.01)	1.27	(0.27)	0.02	(0.90)
$\beta 8$	1.63	(0.22)	13.20	(0.0017)	0.59	(0.45)
$\beta 9$	14.8	(0.001)	2.80	(0.11)	0.45	(0.51)
PC1	19.8	(0.0003)	5.6	(0.03)	0.2	(0.7)

Results of ANCOVA models ($N=22$, $\alpha=0.05$; *P*-values are given in parentheses) predicting the effects of body mass and Zucker rat strain (obese/lean) on the relative abundance of *Tnnt3* splice forms. Inclusion of the interaction term allowed us to examine whether *Tnnt3* splicing responded to body mass change as the severity of obesity progressed.

Of particular interest are *Tnnt3* splice forms $\beta 3$ and $\beta 5$, which showed significant responses to body mass, and highly significant interaction terms indicating obesity effects that were body mass dependent (i.e. depending on the severity of obesity; see Fig. 5B for visual representation of these effects).

The bottom row shows that body mass and obesity had significant effects on PC1 for Zucker rats.

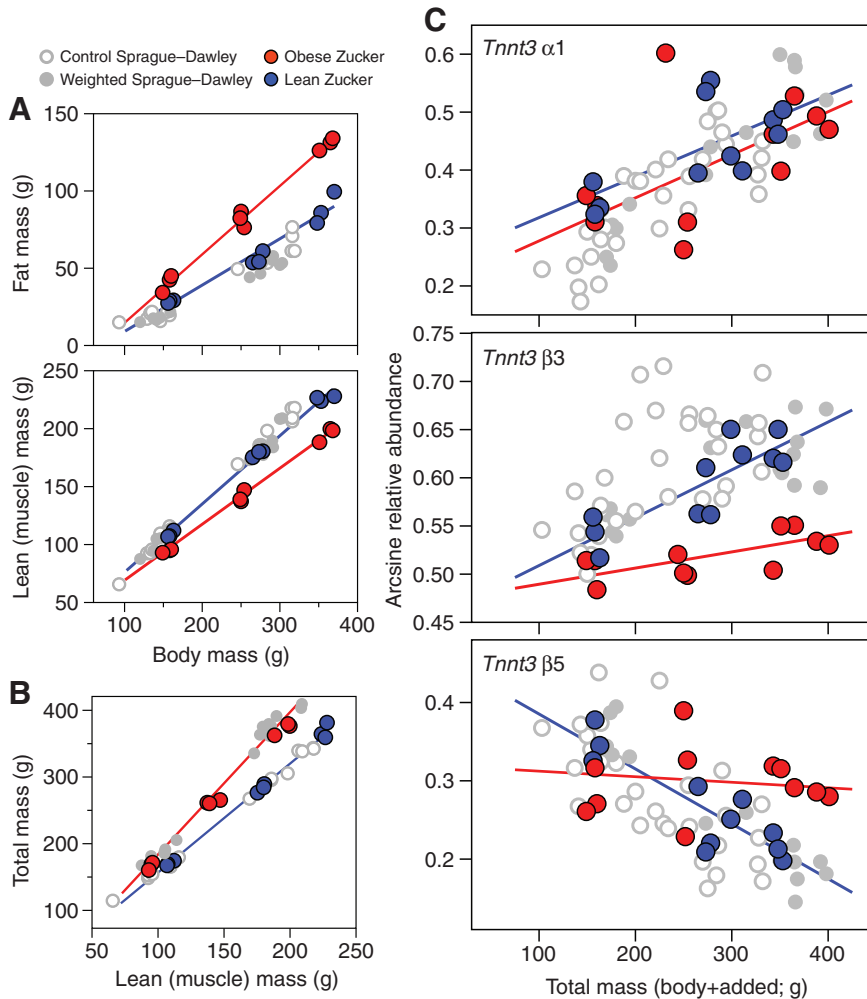


Fig. 5. Body composition and *Tnnt3* splicing response to changes in body weight in lean and obese Zucker rats. Body composition and *Tnnt3* relative abundance data for Zucker rats are superimposed on data for Sprague–Dawley rats. (A) Body fat and lean mass as a function of body mass in male lean and obese Zucker rats ($N=18$). (B) Lean mass contribution to the total weight experienced by skeletal muscles was similar in obese Zucker and weight-loaded Sprague–Dawley rats, indicating that muscles were loaded equally in these groups. (C) Comparison of relative abundance for 3 out of 12 *Tnnt3* splice forms between obese and lean Zucker rats across a range of total mass ($N=22$; see Table 3 for statistical analyses of all *Tnnt3* splice forms). The splicing response to changes in total mass for *Tnnt3* $\alpha 1$ is unaffected by obesity. Impaired responses were observed for *Tnnt3* $\beta 3$ and $\beta 5$ (and $\beta 1$, $\beta 8$ and the first principal component characterizing the overall mixture; see Table 3). The Sprague–Dawley data are shown here only for reference and were excluded from all linear regression fits.

fashion across the two experiments (body composition data are presented in Fig. 5A,B, and statistical comparisons in supplementary material Table S2).

Tnnt3 expression in lean Zucker rats showed the same relationship to total mass as we observed in Sprague–Dawley rats (Fig. 5C). In contrast, obese Zucker rats showed an impaired body weight-dependent response in the β -splice forms (Fig. 5C and Table 3), i.e. those that contain the 3' exon 17, whereas the α -splice forms behaved in the normal fashion. For some of the *Tnnt3* β -splice forms, including the most abundant transcript, *Tnnt3* $\beta 3$, obese rats had a splice form relative abundance normally observed in rats of much lower body mass (e.g. 350 g obese rats had a *Tnnt3* $\beta 3$ relative abundance matching that of 150 g lean rats; Fig. 5C). The mismatch between *Tnnt3* splice form profile and body mass in obese rats increased as body mass increased (e.g. *Tnnt3* $\beta 3$; Fig. 5C and significant interaction effects in Table 3).

The mismatch between *Tnnt3* mRNA splice form profile and body mass in obese rats was accompanied by deviations from the normal troponin T pattern at the protein level (Fig. 6A,B). Large obese Zucker rats showed TNNT3 band patterns that qualitatively resembled those of much smaller Sprague–Dawley and lean Zucker rats (Fig. 6A). Large obese Zucker rats showed an altered relative abundance of TNNT3 bands 2 and 3 compared with large Sprague–Dawley (see also Fig. 3B) and lean Zucker rats (Fig. 6B). For TNNT3 band 1, the pattern shown in Fig. 3B for Sprague–Dawley rats (i.e. decrease with increasing body mass) was

not replicated in a second set of Sprague–Dawley and Zucker rats (Fig. 6). The high variability of this band across the two western blots (Fig. 3B, Fig. 6B) may reflect expression of a mRNA splice form(s) that is not consistently related to body mass (e.g. as we saw at the mRNA level for *Tnnt3* $\beta 2$ or *Tnnt3* $\beta 4$, Table 1).

DISCUSSION

Our findings show that quantitative variation in rat skeletal muscle *Tnnt3* splice form abundance is regulated in response to natural and experimental variation in body weight. This response depends on weight *per se*, rather than on other hidden correlates of body mass, as externally attached weight loads had the same effect as an equal change in body mass due to growth (Fig. 2A). Given the known effect of *Tnnt3* protein isoforms on muscle force and sensitivity to activation by calcium (Brotto, 2005; Gomes et al., 2004; Ogut et al., 1999), the function of this molecular change may be to adjust skeletal muscle mechanical performance in response to load, with consequent effects on force output and energy expenditure during activity (e.g. Table 2). Indeed, the overall *Tnnt3* splicing adjustments associated with body weight gain observed in this study consisted of increases in the relative abundance of *Tnnt3* splice forms that exclude exon 4 (e.g. *Tnnt3* $\alpha 1$ and $\beta 3$), and decreases in those that include exon 4 (e.g. *Tnnt3* $\beta 5$ and $\beta 9$). Reduced inclusion of exon 4 is known to correlate with increased muscle fiber calcium sensitivity (Briggs and Schachat, 1996; Schachat et al., 1987). Hence, we predict that the overall effect of natural and experimental

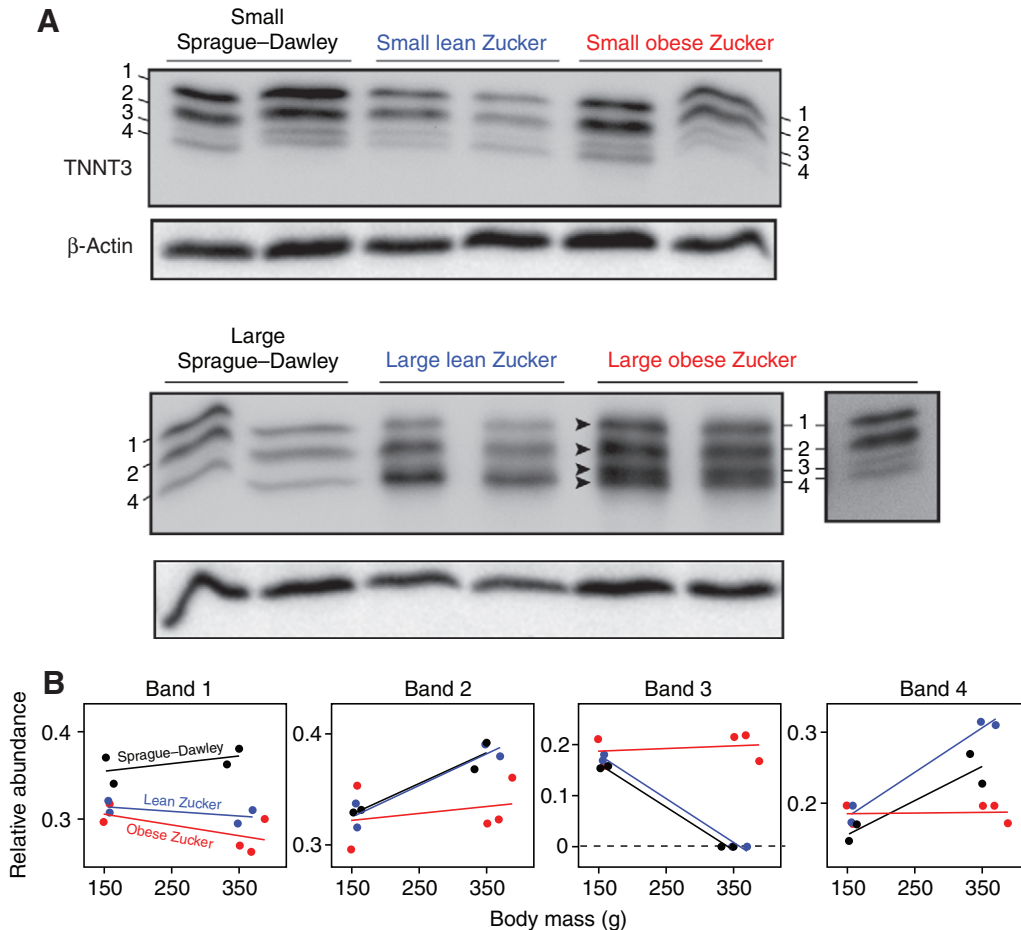


Fig. 6. Weight-associated changes in TNNT3 protein band abundance in Sprague-Dawley and Zucker rat gastrocnemius muscle. (A) A western blot for TNNT3 detected four bands in small rats (i.e. 149–164 g), whereas the large Sprague-Dawley and lean Zucker rats (i.e. 332–370 g) displayed three bands. In large obese Zucker rats (i.e. 351–388 g), an expression pattern similar to that of small rats (i.e. four bands, indicated by black arrowheads) was observed. Upper and lower main panels originate from the same western blot, but are presented separately. β -Actin levels (obtained after stripping and reprobing the same western blot) are provided to demonstrate relatively uniform protein loading. β -Actin levels were not significantly affected by changes in body weight (one-way ANOVA: $F=1.54$, $P=0.243$). The small panel on the lower right of part A originates from a separate western blot and differs in exposure from the two main panels. This panel provides a more readily perceivable visualization of the small rat-like band pattern in large obese Zucker rats, but these band intensities were not used for quantification. (B) Relative abundance of TNNT3 protein bands in relation to body mass for Sprague-Dawley rats and lean and obese Zucker rats. Data fits are provided to demonstrate trends only, as sample sizes are insufficient for statistical inference. Large obese Zucker rat TNNT3 band relative abundance differed from that of Sprague-Dawley and lean Zucker rats for bands 2 and 3 in particular.

increases in body weight is an increased calcium sensitivity and force output in gastrocnemius and perhaps other weight-bearing muscles. We are currently testing these predictions.

In obese Zucker rats, this response was impaired, causing a mismatch between body mass and certain components of skeletal muscle *Tnnt3* composition that became more pronounced as obesity increased (Fig. 5C, Table 3). This mismatch includes *Tnnt3* β 3, β 4, β 5, β 6 and β 8 (Fig. 5C); transcripts that respond to native and/or applied weight loads (except *Tnnt3* β 4, see Table 1), and are associated with nocturnal energy expenditure rate (except *Tnnt3* β 6, see Table 2). For *Tnnt3* β 3– β 5, there were significant interaction effects between body mass and obesity status, indicating that the weight dependency of the relative abundance of these *Tnnt3* splice forms changed as body size increased and obesity progressed. Thus, obese Zucker rats appear to partially, yet progressively, lose the ability to homeostatically regulate their skeletal muscle molecular composition, starting at an early point in the development of obesity.

Moreover, from the previous paragraph it follows that the dramatic reduction of *Tnnt3* β 3 and increase in *Tnnt3* β 5 mRNA

relative abundance (i.e. relatively more exon 4 inclusion in the overall *Tnnt3* splice form pool) in larger obese Zucker rats would lead to decreased calcium sensitivity and hence force output by their gastrocnemius muscles.

The resulting mismatch between body weight and skeletal muscle molecular composition (and presumably performance) may be a component of pathologies common in human obesity, such as chronic muscle weakness, increased load-induced muscle injury and unwillingness to participate in exercise (Anandacoomarasamy et al., 2008; Levine et al., 2005).

Quantitative changes in the *Tnnt3* isoform profile at the mRNA level were paralleled by qualitative changes at the protein level, in both Sprague-Dawley and Zucker rats, including obese Zucker rats. Achieving a more precise understanding of the relationship between transcript and protein expression of this gene is extremely problematic, as the *Tnnt3* α - and β -splice forms differ at the mutually exclusive exon pair near the 3' end, and each exists with varying combinations of alternative exons near the 5' end of the gene. Hence, antibodies specific for α and β proteins would hybridize with a

mixture of different TNNT3 isoforms. For this reason, we have restricted our protein-level analysis of this gene to qualitative and simple quantitative examination.

Zucker rats become obese at an early age because of a genetic impairment in leptin signaling (Bray, 1977), and therefore it remains to be determined whether the effects observed in this study are specific to this model system or are associated generally with the development of obesity *per se*. Investigating the *Tnnt3* splicing response to the development of obesity caused by a high fat diet in otherwise healthy rats will help to clarify this. Nutritional regulation of pre-mRNA alternative splicing has not been examined in great detail (but see Salati and Amir-Ahmady, 2001; Salati et al., 2004) but, interestingly, in addition to body weight, alternative splicing of insect muscle troponin T is sensitive to nutrition (Marden et al., 2008). Moreover, alternative splicing of the vertebrate insulin receptor gene, a key component of nutrient signaling, is co-regulated with that of troponin T (Ho et al., 2004). Hence, it is possible that signals involving energy homeostasis commonly affect the regulation of troponin T splicing.

Research on mechanisms controlling body weight homeostasis has focused primarily on neuroendocrine regulation of food intake, satiety and energy storage depot size (Levin, 2006; McMinn et al., 2000; Morton et al., 2006; Schwartz et al., 2000). In concert with such mechanisms, our results suggest that there may be an important role for the skeletal musculature in maintaining proper body weight homeostasis. Healthy skeletal muscles apparently receive signals (intracellular and/or extracellular) about the amount of load they experience, and respond by changing their *Tnnt3* isoform composition. Elucidating the signaling pathways responsible for this regulatory response may improve our understanding of muscle function and identify targets for therapeutic intervention to reduce muscle pathologies in obesity.

Molecular signaling pathways mediating mechanical load-associated effects on muscle physiology are poorly understood, and have been examined primarily in terms of their involvement in skeletal muscle protein synthesis and growth (e.g. Atherton et al., 2009; Hornberger et al., 2005; Spangenburg, 2009). It is becoming apparent that many alternative splicing events require the activity of the same signaling pathways (Lynch, 2007). For example, the phosphatidylinositol 3-kinase (PI3K)/Akt/mTOR (mammalian target of rapamycin) signaling cascade mediates skeletal muscle protein synthesis in response to nutritional and mechanical stimuli (Anthony et al., 2000; Bolster et al., 2003; Kimball and Jefferson, 2006; Kimball et al., 2000; Sasai et al., 2010), and also activates and interacts with members of the serine/arginine (SR)-rich protein family (Blaustein et al., 2009; Kami et al., 2008; Lynch, 2007), a ubiquitous set of alternative splicing factors that affect exon inclusion/exclusion and facilitate translation of specific mRNAs (Blaustein et al., 2005; Sanford et al., 2005). Modulation of sarcomere gene alternative splicing by nutritional and/or mechanically induced signaling through PI3K/Akt/mTOR would add important functionality to the already complex nature of this pathway, and may mediate the dietary and weight-loading effects on troponin T alternative splicing observed in both insects and mammals.

Impairment of the normal *Tnnt3* splicing response in obese rats is restricted to the β -splice forms (see Fig. 5C and Table 3, i.e. those that contain the 3' exon 17) (Pan and Potter, 1992). This result implies that a particular aspect of the regulation of alternative splicing (i.e. 3' end exon inclusion) is modified during obesity. This specificity may help to guide future examination of the signaling pathways responsible. Obesity is associated with a chronic inflammatory state mediated by the infiltration of adipose tissue by macrophages (Wisse, 2004).

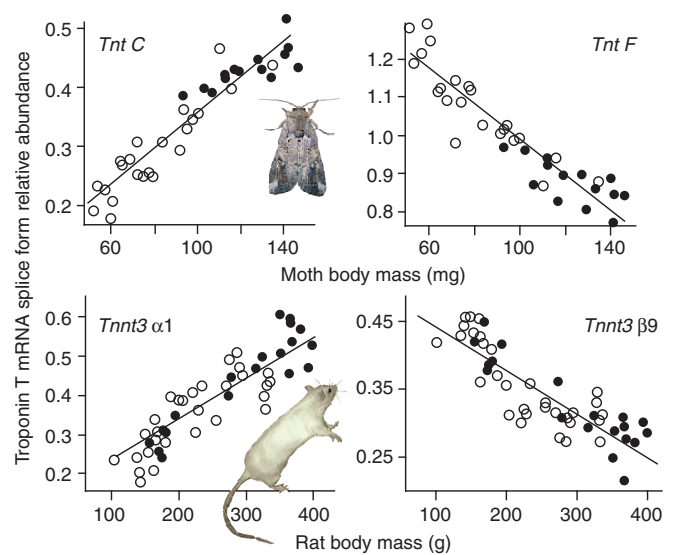


Fig. 7. Comparison of body weight-dependent *troponin T* alternative splicing in insects and mammals. Insects [upper panels; graphs are modified from data originally published in Marden et al. (Marden et al., 2008)] and mammals (lower panels; data from this study) show very similar body weight-dependent reaction norms for the troponin T mRNA splice form profile. In both taxa the response is identical for growth-related changes in body mass (open circles) and experimental weight loading (filled circles). There is not a direct homology of the exon structure of the alternative troponin T mRNA transcripts for which relative abundance is shown here; precisely how these molecular variations affect function in either taxa remains to be determined.

Importantly, inflammation in skeletal muscle impairs splice factor expression (Xiong et al., 2006), and attenuates Akt (Varma et al., 2009) and mTOR signaling (Lang et al., 2007). Indeed, skeletal muscle in rodent models of obesity (including Zucker rats) shows impaired Akt and mTOR signaling (Katta et al., 2009; Kim et al., 2000), which reinforces that idea that these pathways are prime candidates to examine in regard to the impairment in *Tnnt3* splicing we observed.

More broadly, these results indicate that skeletal muscle composition is regulated to accommodate performance requirements associated with changing body weight in a fashion that is evolutionarily conserved in animals ranging from insects (Marden et al., 2008) to mammals (illustrated in Fig. 7). Such a response may be necessary because muscle force scales with cross-sectional area whereas gravitational load scales with body mass. For dimensionally similar animals (i.e. proportions of linear dimensions are invariant), increasing muscle mass alone will not maintain a constant ratio of force to body weight as animals grow larger (Biewener, 1989). The ability to modulate performance by changing muscle *Tnnt3* isoform composition may at least partially circumvent such geometric constraints.

In summary, our findings provide a new mammalian model system to study the quantitative regulation of alternative splicing, and a quantitative marker for an evolutionarily conserved homeostatic mechanism by which animals respond to body weight. Identifying the body weight-sensitive pathways that regulate *Tnnt3* alternative splicing, and the dysregulation thereof during obesity, may reveal new ways to approach the biomedicine of body weight regulation in health and disease.

ACKNOWLEDGEMENTS

The authors thank Dr Ronald P. Wilson for help in developing the weight-loading protocol, Dr Howard W. Fescemeyer for help with *Tnnt3* splice form cloning and

quantification, and Dan A. Brill for help with indirect calorimetry experiments. We also acknowledge the Penn State Genomics Core Facility at University Park, PA, USA, for services provided in *Tnnt3* splice form sequencing and quantification. The studies described herein were supported by funds from the National Institutes of Health DK15658 (to L.S.J.), the National Science Foundation EF-0412651 and IOS-0950416 (to J.H.M.), and the American Physiological Society (Postdoctoral Fellowship in Physiological Genomics to R.J.S.). Deposited in PMC for release after 12 months.

REFERENCES

- Anandacoomarasamy, A., Catterson, I., Sambrook, P., Fransen, M. and March, L. (2008). The impact of obesity on the musculoskeletal system. *Int. J. Obes. (Lond.)* **32**, 2112-2122.
- Anthony, J. C., Yoshizawa, F., Anthony, T. G., Vary, T. C., Jefferson, L. S. and Kimball, S. R. (2000). Leucine stimulates translation initiation in skeletal muscle of postabsorptive rats via a rapamycin-sensitive pathway. *J. Nutr.* **130**, 2413-2419.
- Atherton, P. J., Szewczyk, N. J., Selby, A., Rankin, D., Hillier, K., Smith, K., Rennie, M. J. and Loughna, P. T. (2009). Cyclic stretch reduces myofibrillar protein synthesis despite increases in FAK and anabolic signalling in L6 cells. *J. Physiol.* **587**, 3719-3727.
- Biewener, A. A. (1989). Scaling body support in mammals: limb posture and muscle mechanics. *Science* **245**, 45-48.
- Blaustein, M., Pelisch, F., Tanos, T., Muñoz, M. J., Wengier, D., Quadrana, L., Sanford, J. R., Muschietti, J. P., Kornblitt, A. R., Cáceres, J. F. et al. (2005). Concerted regulation of nuclear and cytoplasmic activities of SR proteins by AKT. *Nat. Struct. Mol. Biol.* **12**, 1037-1044.
- Blaustein, M., Quadrana, L., Rizzo, G., Mata, M. D. L., Pelisch, F. and Srebrow, A. (2009). SF2/ASF regulates proteomic diversity by affecting the balance between translation initiation mechanisms. *J. Cell. Biochem.* **107**, 826-833.
- Bolster, D. R., Kubica, N., Crozier, S. J., Williamson, D. L., Farrell, P. A., Kimball, S. R. and Jefferson, L. S. (2003). Immediate response of mammalian target of rapamycin (mTOR)-mediated signalling following acute resistance exercise in rat skeletal muscle. *J. Physiol.* **553**, 213-220.
- Bray, G. A. (1977). The Zucker-fatty rat: a review. *Fed. Proc.* **36**, 148-153.
- Briggs, M. M. and Schachat, F. (1996). Physiologically regulated alternative splicing patterns of fast troponin T RNA are conserved in mammals. *Am. J. Physiol. Cell Physiol.* **270**, C298-C305.
- Brotto, M. A. (2005). Coupled expression of troponin T and troponin I isoforms in single skeletal muscle fibers correlates with contractility. *Am. J. Physiol. Cell Physiol.* **290**, C567-C576.
- Chandra, M., Tschirgi, M. L., Rajapakse, I. and Campbell, K. B. (2006). Troponin T modulates sarcomere length-dependent recruitment of cross-bridges in cardiac muscle. *Biophys. J.* **90**, 2867-2876.
- Galgani, J. and Ravussin, E. (2008). Energy metabolism, fuel selection and body weight regulation. *Int. J. Obes. Relat. Metab. Disord.* **32** Suppl. 7, S109-S119.
- Goldsmith, R., Joannis, D. R., Gallagher, D., Pavlovich, K., Shamoan, E., Leibel, R. L. and Rosenbaum, M. (2010). Effects of experimental weight perturbation on skeletal muscle work efficiency, fuel utilization, and biochemistry in human subjects. *Am. J. Physiol. Regul. Integr. Comp. Physiol.* **298**, R79-R88.
- Gomes, A. V., Barnes, J. A., Harada, K. and Potter, J. D. (2004). Role of troponin T in disease. *Mol. Cell. Biochem.* **263**, 115-129.
- Greaser, M. L., Moss, R. L. and Reiser, P. J. (1988). Variations in contractile properties of rabbit single muscle fibres in relation to troponin T isoforms and myosin light chains. *J. Physiol.* **406**, 85-98.
- Hartner, K. T., Kirschbaum, B. J. and Pette, D. (1989). The multiplicity of troponin T isoforms. Distribution in normal rabbit muscles and effects of chronic stimulation. *Eur. J. Biochem.* **179**, 31-38.
- Ho, T. H., Charlet, B. N., Poulos, M. G., Singh, G., Swanson, M. S. and Cooper, T. A. (2004). Muscleblind proteins regulate alternative splicing. *EMBO J.* **23**, 3103-3112.
- Hornberger, T. A., Armstrong, D. D., Koh, T. J., Burkholder, T. J. and Esser, K. A. (2005). Intracellular signaling specificity in response to uniaxial vs. multiaxial stretch: implications for mechanotransduction. *Am. J. Physiol. Cell Physiol.* **288**, C185-C194.
- Hulens, M., Vansant, G., Lysens, R., Claessens, A. L., Muls, E. and Brumagne, S. (2001). Study of differences in peripheral muscle strength of lean versus obese women: an allometric approach. *Int. J. Obes. Relat. Metab. Disord.* **25**, 676-681.
- Jackson, A. W., Lee, D.-C., Sui, X., Morrow, J. R., Church, T. S., Maslow, A. L. and Blair, S. N. (2009). Muscular strength is inversely related to prevalence and incidence of obesity in adult men. *Obesity (Silver Spring)* **18**, 1988-1995.
- Karni, R., Hippe, Y., Lowe, S. W. and Krainer, A. R. (2008). The splicing-factor oncoprotein SF2/ASF activates mTORC1. *Proc. Natl. Acad. Sci. USA* **105**, 15323-15327.
- Katta, A., Karkala, S. K., Wu, M., Meduru, S., Desai, D. H., Rice, K. M. and Blough, E. R. (2009). Lean and obese Zucker rats exhibit different patterns of p70s6 kinase regulation in the tibialis anterior muscle in response to high-force muscle contraction. *Muscle Nerve* **39**, 503-511.
- Kemp, J. G., Blazev, R., Stephenson, D. G. and Stephenson, G. M. M. (2009). Morphological and biochemical alterations of skeletal muscles from the genetically obese (ob/ob) mouse. *Int. J. Obes. Relat. Metab. Disord.* **33**, 831-841.
- Kim, Y. B., Peroni, O. D., Franke, T. F. and Kahn, B. B. (2000). Divergent regulation of Akt1 and Akt2 isoforms in insulin target tissues of obese Zucker rats. *Diabetes* **49**, 847-856.
- Kimball, S. R. and Jefferson, L. S. (2006). Signaling pathways and molecular mechanisms through which branched-chain amino acids mediate translational control of protein synthesis. *J. Nutr.* **136**, 227S-231S.
- Kimball, S. R., Jefferson, L. S., Nguyen, H. V., Suryawan, A., Bush, J. A. and Davis, T. A. (2000). Feeding stimulates protein synthesis in muscle and liver of neonatal pigs through an mTOR-dependent process. *Am. J. Physiol. Endocrinol. Metab.* **279**, E1080-E1087.
- Lafortuna, C. L., Maffiuletti, N. A., Agosti, F. and Sartorio, A. (2005). Gender variations of body composition, muscle strength and power output in morbid obesity. *Int. J. Obes. (Lond.)* **29**, 833-841.
- Lang, C. H., Frost, R. A. and Vary, T. C. (2007). Regulation of muscle protein synthesis during sepsis and inflammation. *Am. J. Physiol. Endocrinol. Metab.* **293**, E453-E459.
- Larson, D. E., Ferraro, R. T., Robertson, D. S. and Ravussin, E. (1995). Energy metabolism in weight-stable postobese individuals. *Am. J. Clin. Nutr.* **62**, 735-739.
- Levin, B. E. (2006). Central regulation of energy homeostasis intelligent design: how to build the perfect survivor. *Obesity (Silver Spring)* **14** Suppl. 5, 192S-196S.
- Levine, J. A., Lanningham-Foster, L. M., McCrady, S. K., Krizan, A. C., Olson, L. R., Kane, P. H., Jensen, M. D. and Clark, M. M. (2005). Interindividual variation in posture allocation: possible role in human obesity. *Science* **307**, 584-586.
- Lynch, K. W. (2007). Regulation of alternative splicing by signal transduction pathways. *Adv. Exp. Med. Biol.* **623**, 161-174.
- MacFarland, S. M., Jin, J. P. and Brozovich, F. V. (2002). Troponin T isoforms modulate calcium dependence of the kinetics of the cross-bridge cycle: studies using a transgenic mouse line. *Arch. Biochem. Biophys.* **405**, 241-246.
- Marden, J. H., Fitzhugh, G. H., Wolf, M. R., Arnold, K. D. and Rowan, B. (1999). Alternative splicing, muscle calcium sensitivity, and the modulation of dragonfly flight performance. *Proc. Natl. Acad. Sci. USA* **96**, 15304-15309.
- Marden, J. H., Fitzhugh, G. H., Girgenrath, M., Wolf, M. R. and Girgenrath, S. (2001). Alternative splicing, muscle contraction and intraspecific variation: associations between troponin T transcripts, Ca²⁺ sensitivity and the force and power output of dragonfly flight muscles during oscillatory contraction. *J. Exp. Biol.* **204**, 3457-3470.
- Marden, J. H., Fescemyer, H. W., Saastamoinen, M., Macfarland, S. P., Vera, J. C., Frilander, M. J. and Hanski, I. (2008). Weight and nutrition affect pre-mRNA splicing of a muscle gene associated with performance, energetics and life history. *J. Exp. Biol.* **211**, 3653-3660.
- McMinn, J. E., Baskin, D. G. and Schwartz, M. W. (2000). Neuroendocrine mechanisms regulating food intake and body weight. *Obes. Rev.* **1**, 37-46.
- Medford, R. M., Nguyen, H. T., Destree, A. T., Summers, E. and Nadal-Ginard, B. (1984). A novel mechanism of alternative RNA splicing for the developmentally regulated generation of troponin T isoforms from a single gene. *Cell* **38**, 409-421.
- Morton, G. J., Cummings, D. E., Baskin, D. G., Barsh, G. S. and Schwartz, M. W. (2006). Central nervous system control of food intake and body weight. *Nature* **443**, 289-295.
- Nassar, R., Malouf, N. N., Mao, L., Rockman, H. A., Oakeley, A. E., Frye, J. R., Herlong, J. R., Sanders, S. P. and Anderson, P. A. (2005). cTnT1, a cardiac troponin T isoform, decreases myofibrillar tension and affects the left ventricular pressure waveform. *Am. J. Physiol. Heart Circ. Physiol.* **288**, H1147-H1156.
- Ogut, O., Granzier, H. and Jin, J. P. (1999). Acidic and basic troponin T isoforms in mature fast-twitch skeletal muscle and effect on contractility. *Am. J. Physiol.* **276**, C1162-C1170.
- Pan, B. S. and Potter, J. D. (1992). Two genetically expressed troponin T fragments representing alpha and beta isoforms exhibit functional differences. *J. Biol. Chem.* **267**, 23052-23056.
- Perry, S. (1998). Troponin T: genetics, properties and function. *J. Muscle Res. Cell Motil.* **19**, 575-602.
- Rosenkilde, M., Nordby, P., Nielsen, L. B., Stalknecht, B. M. and Helge, J. W. (2010). Fat oxidation at rest predicts peak fat oxidation during exercise and metabolic phenotype in overweight men. *Int. J. Obes. Relat. Metab. Disord.* **34**, 871-877.
- Salati, L. M. and Amir-Ahmady, B. (2001). Dietary regulation of expression of glucose-6-phosphate dehydrogenase. *Annu. Rev. Nutr.* **21**, 121-140.
- Salati, L. M., Szeszel-Fedorowicz, W., Tao, H., Gibson, M. A., Amir-Ahmady, B., Stabile, L. P. and Hodge, D. L. (2004). Nutritional regulation of mRNA processing. *J. Nutr.* **134**, 2437S-2443S.
- Sanford, J. R., Ellis, J. D., Cazalla, D. and Cáceres, J. F. (2005). Reversible phosphorylation differentially affects nuclear and cytoplasmic functions of splicing factor 2/alternative splicing factor. *Proc. Natl. Acad. Sci. USA* **102**, 15042-15047.
- Sasai, N., Agata, N., Inoue-Miyazu, M., Kawakami, K., Kobayashi, K., Sokabe, M. and Hayakawa, K. (2010). Involvement of PI3K/Akt/TOR pathway in stretch-induced hypertrophy of myotubes. *Muscle Nerve* **41**, 100-106.
- Schachat, F. H., Diamond, M. S. and Brandt, P. W. (1987). Effect of different troponin T-tropomyosin combinations on thin filament activation. *J. Mol. Biol.* **198**, 551-554.
- Schwartz, M. W., Woods, S. C., Porte, D., Seeley, R. J. and Baskin, D. G. (2000). Central nervous system control of food intake. *Nature* **404**, 661-671.
- Spangenburg, E. E. (2009). Changes in muscle mass with mechanical load: possible cellular mechanisms. *Appl. Physiol. Nutr. Metab.* **34**, 328-335.
- Stefancsik, R., Randall, J. D., Mao, C. and Sarkar, S. (2003). Structure and sequence of the human fast skeletal troponin T (TNNT3) gene: insight into the evolution of the gene and the origin of the developmentally regulated isoforms. *Comp. Funct. Genomics* **4**, 609-625.
- Stevens, L., Bozzo, C., Nemirovskaya, T., Montel, V., Falempin, M. and Mounier, Y. (2003). Contractile properties of rat single muscle fibers and myosin and troponin isoform expression after hypergravity. *J. Appl. Physiol.* **94**, 2398-2405.
- Varma, V., Yao-Borengasser, A., Rasouli, N., Nolen, G. T., Phanavanh, B., Starks, T., Gurley, C., Simpson, P., McGehee, R. E., Jr, Kern, P. A. et al. (2009). Muscle inflammatory response and insulin resistance: synergistic interaction between macrophages and fatty acids leads to impaired insulin action. *Am. J. Physiol. Endocrinol. Metab.* **296**, E1300-E1310.
- Wang, J. and Jin, J. P. (1997). Primary structure and developmental acidic to basic transition of 13 alternatively spliced mouse fast skeletal muscle troponin T isoforms. *Gene* **193**, 105-114.
- Wisse, B. E. (2004). The inflammatory syndrome: the role of adipose tissue cytokines in metabolic disorders linked to obesity. *J. Am. Soc. Nephrol.* **15**, 2792-2800.
- Xiong, Z., Shaibani, A., Li, Y.-P., Yan, Y., Zhang, S., Yang, Y., Yang, F., Wang, H. and Yang, X.-F. (2006). Alternative splicing factor ASF/SF2 is down regulated in inflamed muscle. *J. Clin. Pathol.* **59**, 855-861.
- Yu, Z. B., Gao, F., Feng, H. Z. and Jin, J.-P. (2006). Differential regulation of myofibrillar protein isoforms underlying the contractility changes in skeletal muscle unloading. *Am. J. Physiol. Cell Physiol.* **292**, C1192-C1203.